

# Spatial Network Calculus: Toward Deterministic Wireless Networking

Yi Zhong, *Senior Member, IEEE*, Xiaohang Zhou, Ke Feng

**Abstract**—This paper extends the classical network calculus to spatial scenarios, focusing on wireless networks with heterogeneous traffic and varying transmit power levels. Building on spatial network calculus, a prior extension of network calculus to spatial settings, we propose a generalized framework by introducing spatial regulations for stationary marked point processes. The regulations correspond to two key constraints: the total transmit power within a spatial region and the cumulative received power at a receiver. Then we prove the equivalence of ball regulation and shot-noise regulation for stationary marked point processes and establish a universal lower bound on the performance of all network links under these constraints. This framework is applicable to diverse network scenarios, as demonstrated by the analysis of performance guarantees for networks with multi-class users. In addition, we propose an SINR-based power control scheme adapted to user traffic, which ensures differentiated quality of service (QoS) for different user classes. We derive deterministic performance guarantees for all links in complex and heterogeneous wireless networks.

**Index Terms**—Network calculus, performance guarantees, stochastic geometry, point process, deterministic networking.

## I. INTRODUCTION

### A. Motivations

Deterministic networking (DetNet), as a frontier in the field of data transmission, is transitioning from traditional *best-effort* services to *guaranteed-performance* services paradigm [2], [3]. This paradigm shift presents broad application prospects in critical areas such as smart manufacturing and vehicular networks. Yet, expanding the traditional (wired) deterministic networking framework to the wireless domain introduces a series of complex scientific challenges and technical bottlenecks due to the inherent characteristics of wireless communications. These challenges arise primarily from the electromagnetic properties of wireless links and the shared nature of the propagation medium. Unlike the controlled environment of wired networks, wireless propagation is vulnerable to multipath reflections and path obstructions, and the lack of physical isolation results in significant interference issues. Consequently, providing deterministic performance services in wireless network environments is particularly challenging. In light of dynamic changes in service demands, randomness in

channel conditions, unpredictability of resources, and potential network congestion, it is critical to develop new traffic management strategies, channel coding techniques, resource allocation schemes, and congestion control mechanisms. Such developments are crucial to ensure the reliability and controllable delay of data transmission.

The theory of network calculus plays an indispensable role in the design of deterministic networks [4], [5]. Initially developed for wired networks, network calculus introduces envelopes to describe network traffic and services, establishing deterministic upper bounds on network delay and data backlog. However, extending this theory to the wireless network domain presents several critical challenges. The intrinsic characteristics of wireless networks, such as signal attenuation, multipath propagation, and dynamic traffic variations, substantially increase the complexity of guaranteeing deterministic performance. Consequently, traditional network calculus methods are challenging to apply directly to wireless networks.

To address these challenges, a *spatial network calculus* was introduced in [6], which extends the classical network calculus by incorporating the spatial dimension along with the temporal dimension. This advancement offers a novel approach to providing deterministic performance guarantees on all links in wireless networks. The core concept involves using stochastic geometry [7]–[9] to analyze each wireless link in large-scale networks (spatial dimension) and integrating this with classical network calculus methods that focus on individual data packets (temporal dimension). This results in a new set of spatial regulations and methods to ensure deterministic performance in wireless networks. This step shows significant potential for deterministic performance guarantees in wireless networks, particularly in scenarios requiring high reliability and real-time performance, such as autonomous driving, industrial control, and telemedicine.

The spatial regulations introduced in [6] only apply to homogeneous networks, focusing on constraining the number of nodes. It does not capture the heterogeneity of nodes (such as power and density), traffic, and QoS demands in wireless networks [10]. For example, an approach is needed that tailors for both high-demand and low-demand users. While next-generation mobile communication systems such as 6G have made strides in energy efficiency, ultra-reliability, and low latency, ensuring service guarantees for all users in large-scale heterogeneous wireless networks remains a critical and complex challenge [11], [12].

This paper broadens the scope of the spatial network calculus in [6] to provide performance guarantees in heterogeneous networks with varying power levels and traffic types. Our

Yi Zhong and Xiaohang Zhou are affiliated with the School of Electronic Information and Communications at Huazhong University of Science and Technology, Wuhan, China. Ke Feng started this work at INRIA-ENS Paris, France, and is now with Laboratoire ETIS-UMR, CY Cergy Paris Université, ENSEA, CNRS, 8051, Cergy-Pontoise, France.

This research was supported by the National Natural Science Foundation of China (NSFC) grant No. 62471193. Preliminary findings of this work were presented in WiOpt 2024 [1].

The corresponding author is Yi Zhong (yzhong@hust.edu.cn).

approach provides deterministic performance guarantees while accommodating diverse SINR requirements. We offer both theoretical insights, enriching the spatial network calculus framework, and practical strategies for reliable network performance in dynamic wireless environments. To meet the demands of complex traffic and limited resources, we propose and rigorously evaluate customized power control strategies, highlighting the importance of spatial regulation and strategic resource allocation to ensure QoS for all links.

## B. Related Works

Employing an appropriate point process is critical for accurately modeling the spatial distribution of nodes in wireless networks. Poisson point process (PPP) model is commonly used to depict the spatial distribution of network nodes [8], [13]. When transmitters are modeled as PPP and implemented an access control protocol like Carrier Sense Multiple Access (CSMA), the effective transmitters are modeled as a Matérn hardcore point process (MHCPP) [14], [15]. In [16], an extension of MHCPP is used, where the competition is based on pair-wise SIR protection zones with the modification to the RTS/CTS mechanism which defines a receiver-centered protection zone to restrict other transmitters' activity within the area. Mishra et al. [17] employ stochastic geometry to realistically model automotive radar interference, incorporating the Matérn point process to account for the spatial mutual exclusion of vehicles. Di Renzo et al. [18] use MHCPP for modeling base stations within cellular networks. Chen [19] analyzes the stable packet arrival rate region in discrete-time slotted random access network by arranging the transmitters as MHCPP.

Most existing literature focuses on improving the performance of wireless networks including link success probability, rate, and latency. Miao [20] proposes a joint power control algorithm with QoS guarantee using the convex optimization method that satisfies the minimum rate constraint of the delay-constrained service and the proportional fairness of the best-effort service. Liu's research [21] proposes an algorithm that not only enhances the utility for best-effort users but also diminishes the outage probability for rate-constrained users. In scenarios where resource availability is constrained, the allocation of priority becomes a critical consideration. Choi et al. [22] suggest a mechanism where vehicles engage in transmission based on the highest requirement among their neighboring vehicles. Kumar and colleagues [23] introduce a method for assigning terminal requirements, factoring in both the ongoing service and the terminal location. Abdel-Hadi [24] focuses on finding the optimal solution for the resource allocation problem that includes users with requirements. Lee's work [25] delves into the realm of optimal power control, prioritizing services and thereby directing power control in alignment with these requirements. In [23]–[25], the authors focused on the multi-priority mechanisms and power resource allocation strategies in communication networks, which improve performance and fairness to terminal users.

However, the link performance of all may not be deterministically guaranteed previously due to uncontrolled transmitter

locations. By contrast, we consider spatially regulated point processes, which is inspired by the classical network calculus framework [4], [26], [27]. The seminal work of Cruz in classical network calculus introduces the  $(\sigma, \rho)$  traffic regulation, where  $\sigma$  represents an allowable level of initial burstiness, and  $\rho$  sets the upper limit for the long-term average rate. Thus, traffic flow is bounded by a baseline constant  $\sigma$  and an additional rate  $\rho$  scales the duration of the time interval [4]. As a significant derivative branch of network calculus, stochastic network calculus provides precise quantitative methods for the statistical limits of network performance, marking a new milestone in the development of the theory [28]. In his comprehensive review of stochastic network calculus, Y. Jiang introduced two key concepts: the stochastic arrival curve and the stochastic service curve [29]. These concepts have been fundamental in the study of service guarantee theories and have laid the theoretical groundwork for ensuring deterministic network performance. C.-S. Chang and J.-Y. Le Boudec have summarized advances in the study of queue lengths, packet loss rates, and traffic characteristics in the packet queuing process within stochastic network calculus [27], [30]. In recent years, academic research on network calculus theory has also made significant advancements [31]–[35].

Expanding these principles into spatial contexts, [6] applies the parameters  $\sigma$ ,  $\rho$ , and an additional parameter  $\nu$  to govern the number of wireless links, the cumulative received power, and the interference within large-scale wireless networks. This methodology leads to the development of  $(\sigma, \rho, \nu)$ -ball regulation and  $(\sigma, \rho, \nu)$ -shot-noise regulation in spatial network calculus. In this work, we extend these regulations to provide a methodology to ensure service guarantees for diverse and heterogeneous network scenarios. Furthermore, our research proposes a power control scheme. This scheme is specifically designed to manage the allocation of power in a bipolar network architecture [36], where the transmitters follows a hardcore process, and takes into account the presence of users or traffic of varying requirements.

## C. Contributions

Our work extends the classical network calculus framework to spatial domains with generalized power and interference constraints, enhancing its applicability to practical and complex wireless network scenarios. The key contributions of this paper are as follows.

- We extend two regulatory constraints, i.e., ball regulation and shot-noise regulation, to marked point processes and prove their equivalence in this context. These regulations provide a unified theoretical foundation for deriving performance lower bounds applicable to all network links in complex and heterogeneous wireless networks.
- We develop a generalized framework that provides deterministic guarantees on network performance, including lower bounds for link success probability under diverse user and traffic demands.
- To demonstrate the practical utility of the proposed framework, we analyze a traffic-adaptive power control strategy tailored to heterogeneous traffic conditions. Although this strategy serves as an illustrative example, it

highlights how our results can guide power control to meet varying QoS requirements.

This paper is organized as follows. Section II introduces spatial regulations to govern wireless network configurations. Section III presents a heterogeneous traffic example and derives link success probability lower bounds for all links based on these regulations. Numerical results are discussed in Section IV, followed by conclusions in Section V.

## II. SPATIAL REGULATIONS

For point processes without spatial regulations, such as the PPP, obtaining a lower bound for link success probability or guaranteeing deterministic performance for all links is not feasible due to unbounded interference from nearby transmitters. In contrast, by applying spatial regulations, such as thinning a PPP into a hard-core point process, we can establish upper bounds for both total transmitter power and the total received power within any area. Introducing spatial exclusion between nodes serves as a spatial regulation, enabling a link success probability lower bound across the network. In this section, we will define ball regulation and shot noise regulation for stationary marked point processes and explain their physical significance.

### A. Definitions

To enhance the guaranteed lower bound of network performance, we introduce regulations on power control. We first define the strong version of these regulations, which must be universally applicable across the entire space. In contrast, the weak version requires that the regulations be satisfied only within the context of a jointly stationary point process.

Consider a stationary marked point process  $\Phi = \{(x, P_x)\}$  on  $\mathbb{R}^2 \times \mathbb{R}^+$ , defined on the probability space  $(\Omega, \mathcal{A}, \mathbb{P})$ . Here,  $\Phi = \{x : (x, P_x) \in \tilde{\Phi}\}$  represents the set of transmitter locations and  $P_x > 0$  denotes the transmit power of the transmitter  $x \in \Phi$ .<sup>1</sup> Let  $P_{\text{total}}(y, r) \triangleq \sum_{x \in \Phi \cap B(y, r)} P_x$  denote the total power allocated to all transmitters within  $B(y, r)$ , an open ball of radius  $r$  centered at  $y \in \mathbb{R}^2$ . If  $y$  is arbitrarily chosen in space, we obtain the strong regulations; if  $y$  is selected based on another jointly stationary point process, we obtain the weak regulations. In this work, we use the term ‘‘a.s.’’ (almost surely) to indicate that an event occurs with probability 1.

With these notations in place, we can now define the strong and weak  $(\sigma, \rho, \nu)$ -ball regulations for the stationary marked point process as follows.

**Definition 1.** (Strong  $(\sigma, \rho, \nu)$ -ball regulation). A stationary marked point process  $\tilde{\Phi}$  is said to exhibit strong  $(\sigma, \rho, \nu)$ -ball regulation if, for all  $r \geq 0$ ,

$$P_{\text{total}}(o, r) \leq \sigma + \rho r + \nu r^2, \quad \mathbb{P}\text{-a.s.}, \quad (1)$$

where  $\sigma, \rho, \nu$  are non-negative constants.

Alternatively, one can write (1) as  $\mathbb{P}(P_{\text{total}}(o, r) \leq \sigma + \rho r + \nu r^2) = 1$ . Due to the stationarity of the marked point process,

<sup>1</sup>It is worth noting that marks can represent properties other than transmit power, in which case the results presented in this work remain valid.

the probability distribution of  $P_{\text{total}}(y, r)$  is identical to that of  $P_{\text{total}}(o, r)$  for all  $y \in \mathbb{R}^2$  and  $r > 0$ .

**Definition 2.** (Weak  $(\sigma, \rho, \nu)$ -ball regulation). A stationary marked point process  $\tilde{\Phi}$  exhibits weak  $(\sigma, \rho, \nu)$ -ball regulation with respect to a jointly stationary point process  $\Psi$  if, for all  $r \geq 0$ ,

$$P_{\text{total}}(o, r) \leq \sigma + \rho r + \nu r^2, \quad \mathbb{P}_{\Psi}^o\text{-a.s.}, \quad (2)$$

where  $P_{\text{total}}(o, r) = \sum_{x \in \Phi \cap B(o, r)} P_x$  represents the total power allocated to transmitters within a circular area of radius  $r$ , centered a given point  $o \in \Psi$ , and  $\sigma, \rho, \nu$  are non-negative constants.  $\mathbb{P}_{\Psi}^o$  denotes the Palm probability of  $\Psi$ . If  $\Phi$  is independent of  $\Psi$ , then we get strong regulations.

**Remark 1.** In Definitions 1 and 2,  $\sigma$  represents the maximum power level for all transmitters.  $\rho$  scales linearly with the radius  $r$  of the region, reflecting the contribution to power from the periphery. Meanwhile,  $\nu$  scales quadratically with  $r$ , accounting for the increase in total power proportional to the size of the ball, which is also influenced by the repulsion between transmitters.

**Remark 2.** When the transmit power of all transmitters in  $\Phi$  is equal and normalized to 1, i.e.,  $P_x \equiv 1$  for all  $x \in \Phi$ , we have  $P_{\text{total}}(o, r) = \sum_{x \in \Phi \cap B(o, r)} 1 = \Phi(B(o, r))$ , where  $\Phi(B(o, r))$  denotes the number of points in  $\Phi$  within  $B(o, r)$ . This leads to the inequality:

$$\Phi(B(o, r)) \leq \sigma + \rho r + \nu r^2, \quad \mathbb{P}\text{-a.s.} \quad (3)$$

In this case, the ball regulation for a marked point process is consistent with the definition of ball regulation introduced in [6], which governs the total number of points in a point process within a specified circular region.

We derive the superposition property of the proposed ball regulations.

**Lemma 1.** Consider a stationary marked point process  $\tilde{\Phi}$  constructed as the superposition of  $M$  jointly stationary marked subprocesses  $\tilde{\Phi}_i$ , such that  $\tilde{\Phi} = \bigcup_{i=1}^M \tilde{\Phi}_i$ . If each subprocess  $\tilde{\Phi}_i$  is strongly (or weakly)  $(\sigma_i, \rho_i, \nu_i)$ -ball regulated, then the superposition marked point process  $\tilde{\Phi}$  is also strongly (or weakly)  $(\sigma, \rho, \nu)$ -ball regulated, where

$$\sigma \triangleq \sum_{i=1}^M \sigma_i, \quad \rho \triangleq \sum_{i=1}^M \rho_i, \quad \text{and} \quad \nu \triangleq \sum_{i=1}^M \nu_i. \quad (4)$$

*Proof.* Let  $\Phi_i(B(o, r))$  represent the number of transmitters from the  $i$ -th subprocess within  $B(o, r)$ .

Denote by  $P_{\text{total},i}(o, r)$  the total power of the transmitters of the  $i$ -th subprocess within  $B(o, r)$ . Since each subprocess  $\tilde{\Phi}_i$  is strongly (or weakly)  $(\sigma_i, \rho_i, \nu_i)$ -ball regulated, there exists a upper limit on the total power for all transmitters in the  $i$ -th subprocess within  $B(o, r)$ , i.e.,

$$P_{\text{total},i}(o, r) \leq \sigma_i + \rho_i r + \nu_i r^2, \quad \mathbb{P}\text{-a.s.} \quad (5)$$

Considering the marked point process  $\tilde{\Phi}$ , let  $P_{\text{total}}(o, r)$  denote the total power of transmitters across all subprocesses within the circular region of radius  $r$ ,  $P_{\text{total}}(o, r) \triangleq \sum_{i=1}^M P_{\text{total},i}(o, r)$ .

By substituting (5) into (II-A), we obtain

$$P_{\text{total}}(o, r) \leq \sigma + \rho r + \nu r^2, \quad \mathbb{P}\text{-a.s.} \quad (6)$$

□

Using the above definition of ball regulations, we derive the following lemma, which describes the properties of ball regulation in a type II MHCPP marked with transmit power. A type II MHCPP is a point process that models the spatial distribution of transmitters with mutual exclusion, ensuring that no two transmitters are closer than a specified hardcore distance  $H$ .

In a type II MHCPP, each transmitter is associated with a random timestamp that determines its activation. When a potential transmitter conflicts with others (i.e., if it falls within the hardcore distance of an already active transmitter), it is removed from the process based on its timestamp. Specifically, among the conflicting transmitters, the one with the earliest timestamp is retained, whereas all the others are discarded. This mechanism allows for a higher average density of active transmitters compared to a Type I MHCPP, where all conflicting transmitters are removed simultaneously. The Type II MHCPP is particularly suitable for modeling scenarios such as CSMA protocols, where the timing of transmissions plays a crucial role in minimizing interference.

**Lemma 2.** *A type-II MHCPP on  $\mathbb{R}^2$  with a hardcore distance  $H$ , marked by a constant transmit power  $P$ , is strongly  $\left(P, \frac{2\pi P}{\sqrt{12}H}, \frac{\pi P}{\sqrt{12}H^2}\right)$ -ball regulated.*

*Proof.* Consider the densest packing scenario of the type-II MHCPP (see Fig. 1) on  $\mathbb{R}^2$ , where  $N(r) \triangleq \Phi(B(o, r))$  denotes the total number of transmitters within a radius region  $r$ , and  $H$  represents the hard-core distance. The hardcore condition enforces a minimum distance  $H$  between any two transmitters, with the theoretical maximum density of a hardcore packing in  $\mathbb{R}^2$  being  $\frac{\pi}{\sqrt{12}}$ .

The upper bound of  $N(r)$  for  $r \geq H$  is given by the area of a circle with radius  $r + H$ , divided by the area required per transmitter:

$$\pi H^2 N(r) \leq \frac{\pi^2 (r + H)^2}{\sqrt{12}}. \quad (7)$$

Expanding and rearranging this expression, and applying  $P_{\text{total}}(o, r) = N(r)P$ , we get:

$$P_{\text{total}}(o, r) \leq P + \frac{2\pi P}{\sqrt{12}H} r + \frac{\pi P}{\sqrt{12}H^2} r^2. \quad (8)$$

Due to the stationarity, we obtain the result in the lemma. □

**Remark 3.** *Lemma 2 states that a type II MHCPP with constant transmit power mark  $P$  is strongly ball regulated, with the upper bound specified in (8) holding for any circular area of radius  $r$  centered at an arbitrarily chosen point in space. If these centers are selected based on a jointly stationary point process  $\Psi$ , the condition in (8) remains valid. Consequently, a type II MHCPP with a hardcore distance  $H$  and constant transmit power mark  $P$  is also weakly  $\left(P, \frac{2\pi P}{\sqrt{12}H}, \frac{\pi P}{\sqrt{12}H^2}\right)$ -ball regulated with respect to any stationary point process.*

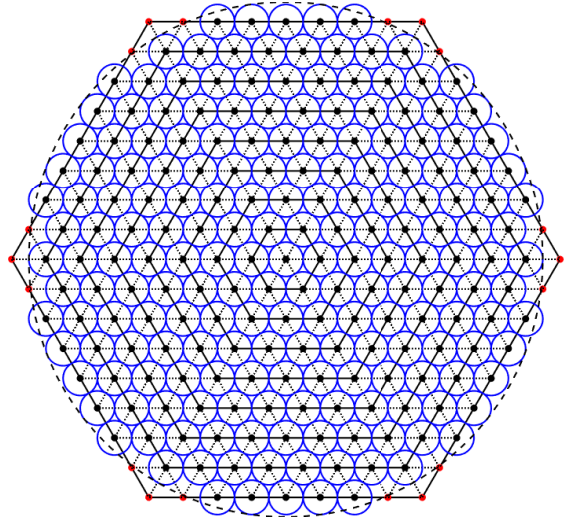


Fig. 1. Diagram of a triangular lattice with eight hexagonal rings of nodes in wireless network. Solid dots represent transmitters, blue circles represent guard zones with a radius of the hardcore distance  $H$ , and all retained transmitters are located within a dashed circle with radius  $r$ . Ring  $k$  contains  $6k$  nodes [37].

In addition to regulating total power within a circular region, we also impose regulations on the power of shot noise.

**Definition 3.** (*Strong  $(\sigma, \rho, \nu)$ -shot-noise regulation*). A stationary marked point process  $\Phi$  is strongly  $(\sigma, \rho, \nu)$ -shot-noise regulated if, for all non-negative, bounded, and non-increasing functions  $\ell : \mathbb{R} \rightarrow \mathbb{R}$  and for all  $R > 0$ ,

$$\begin{aligned} \sum_{x \in \Phi \cap B(o, R)} P_x \ell(\|x\|) &\leq \sigma \ell(0) \\ &+ \rho \int_0^R \ell(r) dr + 2\nu \int_0^R r \ell(r) dr, \quad \mathbb{P}\text{-a.s.}, \end{aligned} \quad (9)$$

where  $\|x\|$  denotes the Euclidean norm of the vector  $x$ .

By the stationarity of the marked point process  $\tilde{\Phi}$ , (9) holds for any  $y \in \mathbb{R}^2$  as:

$$\begin{aligned} \sum_{x \in \Phi \cap B(y, R)} P_x \ell(\|x - y\|) &\leq \sigma \ell(0) + \rho \int_0^R \ell(r) dr \\ &+ 2\nu \int_0^R r \ell(r) dr, \quad \mathbb{P}\text{-a.s.} \end{aligned} \quad (10)$$

If  $y$  is chosen from another point process  $\Psi$  rather than arbitrarily from the whole space  $\mathbb{R}^2$ , we obtain the weak version of the shot-noise regulation, defined as follows.

**Definition 4.** (*Weak  $(\sigma, \rho, \nu)$ -shot-noise regulation*). A stationary marked point process  $\tilde{\Phi}$  is said to be weakly  $(\sigma, \rho, \nu)$ -shot-noise regulated with respect to  $\Psi$  if, for all non-negative, bounded, and non-increasing functions  $\ell : \mathbb{R}^+ \rightarrow \mathbb{R}^+$ , for all  $R > 0$ , and for all  $y \in \Psi$ ,

$$\begin{aligned} \sum_{x \in \Phi \cap B(o, R)} P_x \ell(\|x\|) &\leq \sigma \ell(0) + \rho \int_0^R \ell(r) dr \\ &+ 2\nu \int_0^R r \ell(r) dr, \quad \mathbb{P}_{\Psi}^o\text{-a.s.} \end{aligned} \quad (11)$$

When the transmit power is constant and normalized to 1, i.e.,  $P_x = 1$  for all  $x \in \Phi$ , the  $(\sigma, \rho, \nu)$ -shot-noise regulation reduces to the  $(\sigma, \rho, \nu)$ -shot-noise regulation presented in [6].

By considering the special case where the function  $\ell(\cdot)$  is identically equal to 1, we obtain a formulation analogous to the  $(\sigma, \rho, \nu)$ -ball regulation for all  $R > 0$ , expressed as:

$$P_{\text{total}}(o, R) \leq \sigma + \rho R + \nu R^2, \quad \mathbb{P}\text{-a.s.} \quad (12)$$

**Remark 4.** As  $R \rightarrow +\infty$ , (9) simplifies to:

$$\sum_{x \in \Phi} P_x \ell(\|x\|) \leq A_\ell, \quad \mathbb{P}\text{-a.s.}, \quad (13)$$

where

$$A_\ell \triangleq \sigma \ell(0) + \rho \int_0^\infty \ell(r) dr + 2\nu \int_0^\infty r \ell(r) dr \quad (14)$$

represents the asymptotic upper bound on the total weighted sum of all points in  $\Phi$ , weighted by the function  $\ell$  and the transmit power  $P_x$ .

The physical meaning of the  $(\sigma, \rho, \nu)$ -shot-noise regulation is that it describes how the power dynamics operate within a spatially distributed network. Specifically, for a user at the origin, this regulation governs the cumulative impact of both useful signal power and interference from other transmitters. The total impact is bounded by the parameters  $\sigma$ ,  $\rho$ , and  $\nu$ . These constraints are functionally implemented through the path loss function  $\ell(\cdot)$ , which models the decay of signal strength with distance in wireless networks.

The relationship between ball regulation and shot-noise regulation is established in the following theorem, which states their equivalence.

**Theorem 1.** A stationary marked point process  $\tilde{\Phi}$  is strongly  $(\sigma, \rho, \nu)$ -shot-noise regulated if and only if it is strongly  $(\sigma, \rho, \nu)$ -ball regulated.

*Proof.* To prove that strong  $(\sigma, \rho, \nu)$ -shot-noise regulation implies strong  $(\sigma, \rho, \nu)$ -ball regulation, we set the weight function  $\ell(\cdot) \equiv 1$  for all  $r \geq 0$  in (9). The shot-noise regulation simplifies to the total power allocated to all transmitters in  $B(o, r)$ , bounded as:

$$P_{\text{total}}(o, r) = \sum_{x \in \Phi \cap B(o, r)} P_x \leq \sigma + \rho r + \nu r^2, \quad \mathbb{P}\text{-a.s.} \quad (15)$$

Thus, strong  $(\sigma, \rho, \nu)$ -ball regulation holds.

To prove that strong  $(\sigma, \rho, \nu)$ -ball regulation implies strong  $(\sigma, \rho, \nu)$ -shot-noise regulation, for  $R > 0$ , we partition the open ball  $B(o, R)$  into  $n$  concentric annuli with radii  $r_k = k\Delta$ , where  $\Delta \triangleq R/n$ ,  $n \in \mathbb{N}$ , and  $k = 0, 1, \dots, n$ . Let  $B_k \triangleq B(o, r_k)$ , and denote the value of the weight function  $\ell(r)$  at

radius  $r_k$  as  $l_k \triangleq \ell(r_k)$ . The shot-noise generated by  $\ell$  within  $B(o, R)$  is

$$\begin{aligned} & \sum_{x \in \Phi \cap B(o, R)} P_x \ell(\|x\|) \\ & \stackrel{(a)}{=} \sum_{k=1}^n \sum_{x \in \Phi \cap (B_k \setminus B_{k-1})} P_x \ell(\|x\|) \\ & \stackrel{(b)}{\leq} \sum_{k=1}^n \sum_{x \in \Phi \cap (B_k \setminus B_{k-1})} P_x l_{k-1} \\ & \stackrel{(c)}{=} \sum_{k=1}^n l_{k-1} (P_{\text{total}}(o, r_k) - P_{\text{total}}(o, r_{k-1})). \end{aligned} \quad (16)$$

- Step (a): The sum over the circular area  $B(o, R)$  is partitioned into sums over the annular regions  $B_k \setminus B_{k-1}$ .

- Step (b): The inequality follows from the monotonicity of  $\ell(r)$ , which ensures that  $\ell(\|x\|) \leq l_{k-1}$  for  $x \in B_k \setminus B_{k-1}$ .

- Step (c): The summation over each annular region reduces to the difference in cumulative power between  $P_{\text{total}}(o, r_k)$  and  $P_{\text{total}}(o, r_{k-1})$ .

As  $n \rightarrow \infty$ , the summation converges to the Riemann-Stieltjes integral:

$$\int_0^R \ell(r) dP_{\text{total}}(o, r), \quad (17)$$

since  $P_{\text{total}}(o, r)$  is bounded, non-decreasing, and integrable on  $\mathbb{R}^2$ . This integral can be expanded using integration by parts:

$$\begin{aligned} & \int_0^R \ell(r) dP_{\text{total}}(o, r) \\ & = \ell(R)P_{\text{total}}(o, R) - \ell(0)P_{\text{total}}(o, 0) - \int_0^R P_{\text{total}}(o, r) d\ell(r) \\ & \stackrel{(a)}{\leq} \ell(R) (\sigma + \rho R + \nu R^2) - \int_0^R (\sigma + \rho r + \nu r^2) d\ell(r) \\ & = \sigma \ell(0) + \rho \int_0^R \ell(r) dr + 2\nu \int_0^R r \ell(r) dr, \quad \mathbb{P}\text{-a.s.} \end{aligned} \quad (18)$$

In step (a), the inequality uses the assumption that  $\Phi$  is strongly  $(\sigma, \rho, \nu)$ -ball regulated, bounding  $P_{\text{total}}(o, R)$ . The proof is complete.  $\square$

Similarly, we get the following corollary, which states the equivalence for weak regulations.

**Corollary 1.** A stationary marked point process  $\tilde{\Phi}$  is weakly  $(\sigma, \rho, \nu)$ -shot-noise regulated with respect to a jointly stationary point process  $\Psi$  if and only if it is weakly  $(\sigma, \rho, \nu)$ -ball regulated with respect to  $\Psi$ .

*Proof.* Apply the techniques in the proof of Theorem 1.  $\square$

## B. Performance Bounds

In our study, we focus on two channel models: Rayleigh fading and the absence of fading. The analysis can be easily generalized to general fading [6]. Without loss of generality, we consider a receiver located at the origin, with its dedicated

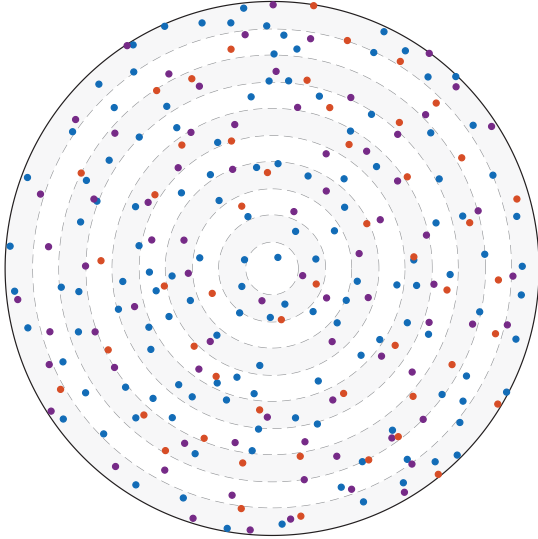


Fig. 2. Illustration of a circular area with radius  $R = 15$ , displaying the spatial distribution of transmitters operating at three distinct power levels. The circular region is divided into  $n = 10$  concentric annular regions, each with a spacing of  $\Delta = R/n = 1.5$ . Transmitters are represented by solid dots, with orange, purple, and blue dots corresponding to high-power, medium-power, and low-power transmitters, respectively. The transmitter locations are initially generated using a PPP with an intensity  $\lambda = 0.3$ , and then filtered to form a type II MHCPP. The resulting minimum separation distances (hardcore distances) are  $H_1 = 1$  for high-power transmitters,  $H_2 = 0.8$  for medium-power transmitters, and  $H_3 = 0.5$  for low-power transmitters. The dashed lines indicate the boundaries of the annular regions used for analytical segmentation in the proof process.

transmitter positioned at  $x_0$ . Let  $r_0$  denote the distance from the receiver to its dedicated transmitter  $x_0$ , i.e.,  $r_0 = \|x_0\|$ .

Using a bounded, non-increasing, continuous, and integrable function  $\ell(r)$  as the path loss function, we can express the SINR for the receiver as

$$\text{SINR} = \frac{P_{x_0} h_{x_0} \ell(r_0)}{I + W}, \quad (19)$$

where  $P_{x_0}$  is the transmit power of the transmitter at  $x_0$ ,  $W$  is the variance of the additive white Gaussian noise, and  $I$  is the interference power from other signals in the network expressed as

$$I = \sum_{x \in \Phi \setminus \{x_0\}} P_x h_x \ell(\|x\|). \quad (20)$$

We denote  $h_x$  as the small-scale fading coefficient from the transmitter located at position  $x$  to its corresponding receiver. In the absence of fading, we set  $h_x = 1$  for all transmitters, which simplifies the SINR expression. When considering channel fading, we adopt a Rayleigh fading model, where the fading coefficients are independent and identically distributed (i.i.d.). In this case, the power attenuation  $h_x$  follows an exponential distribution with unit mean, i.e.,  $h_x \sim \text{Exp}(1)$ .

**Theorem 2.** *When a stationary marked point process  $\tilde{\Phi}$  is either strongly  $(\sigma, \rho, \nu)$ -ball regulated or weakly  $(\sigma, \rho, \nu)$ -ball regulated with respect to the receiver point process, and in the absence of channel fading (i.e.,  $h_x \equiv 1$ ), the interference*

*conditioned on the transmit power  $P_{x_0}$  at  $x_0$  can be almost surely bounded as*

$$I \leq A_\ell - P_{x_0} \ell(r_0), \quad \mathbb{P}\text{-a.s.} \quad (21)$$

*Consequently, an almost sure lower bound for the SINR, conditioned on the transmit power  $P_{x_0}$ , is given by*

$$\text{SINR} \geq \frac{\theta P_{x_0} \ell(r_0)}{A_\ell - P_{x_0} \ell(r_0)}, \quad \mathbb{P}\text{-a.s.} \quad (22)$$

*Proof.* Since the transmitter marked point process  $\tilde{\Phi}$  is  $(\sigma, \rho, \nu)$ -ball regulated. Due to the equivalence between ball regulation and shot-noise regulation established in Theorem 1 and Corollary 1, we conclude that the marked point process  $\tilde{\Phi}$  is also  $(\sigma, \rho, \nu)$ -shot-noise regulated.

In a scenario without channel fading (i.e.,  $h_x = 1$ ), the interference experienced by a user can be bounded using (13) as (21). Given this upper bound on interference, we can derive further almost sure lower bounds for SINR in (22).  $\square$

Considering the case with channel fading, for a target SINR thresholds  $\theta > 0$ , the link success probability can be denoted by

$$P_s(\theta | \tilde{\Phi}) \triangleq \mathbb{P}(\text{SINR} > \theta | \tilde{\Phi}), \quad (23)$$

where  $P_s(\theta | \tilde{\Phi}) \in [0, 1]$  is a random variable conditioned on the locations and the transmit powers of all transmitters. Link success probability can be interpreted as the probability that the SINR of a link with its user located at the origin exceeds the threshold  $\theta$ , given a network and power control realization  $\tilde{\Phi}$ , and accounting for the effects of fading. The distribution associated with  $P_s(\theta | \tilde{\Phi})$  is known as the *meta distribution* [38], [39].

Although the link success probability  $P_s(\theta | \tilde{\Phi})$  is subject to randomness due to fading, a definite lower bound  $\gamma_0$  can be established such that

$$\mathbb{P}\left(P_s(\theta | \tilde{\Phi}) > \gamma_0\right) = 1. \quad (24)$$

This value,  $\gamma_0$ , is termed the success probability lower bound for all links. Similarly, if we require that 80% of the links meet the SINR threshold requirement, it can be expressed as  $\mathbb{P}\left(P_s(\theta | \tilde{\Phi}) > \gamma_0\right) = 0.8$ .

The challenge then is to determine how to achieve a deterministic lower bound  $\gamma_0$  for all links within a large-scale wireless network through our proposed regulatory measures.

**Theorem 3.** *Considering Rayleigh fading, if a stationary marked point process  $\tilde{\Phi}$  is  $(\sigma, \rho, \nu)$ -shot-noise regulated, then the link success probability given the transmit power  $P_{x_0}$  at  $x_0$  satisfies*

$$P_s(\theta | \tilde{\Phi}) \geq \exp\left(-\frac{\theta(W + A_\ell)}{P_{x_0} \ell(r_0)} + \theta\right), \quad \mathbb{P}\text{-a.s.}, \quad (25)$$

where  $A_\ell$  is defined in (14).

*Proof.* For users with a target SINR threshold  $\theta > 0$  in Rayleigh fading channels, the link success probability as given by (23) is expressed as

$$\begin{aligned} P_s(\theta | \tilde{\Phi}) &\stackrel{(a)}{=} \mathbb{P} \left[ \frac{P_{x_0} h_{x_0} \ell(r_0)}{I + W} > \theta \mid \tilde{\Phi} \right] \\ &\stackrel{(b)}{=} \mathbb{E} \left[ \exp \left( -\frac{\theta(I + W)}{P_{x_0} \ell(r_0)} \right) \mid \tilde{\Phi} \right], \end{aligned} \quad (26)$$

where (a) follows from the definition of SINR, and (b) utilizes the property that  $h_x$ , the small-scale fading factor, is exponentially distributed. Here,  $(x_0, P_{x_0}) \in \tilde{\Phi}$ , where  $x_0$  represents the designated transmitter for the receiver located at the origin, and  $P_{x_0}$  denotes its transmit power.

The link success probability can be derived as

$$\begin{aligned} P_s(\theta | \tilde{\Phi}) &= \exp \left( -\frac{\theta W}{P_{x_0} \ell(r_0)} \right) \\ &\times \mathbb{E} \left[ \exp \left( -\frac{\theta \sum_{(x, P_x) \in \tilde{\Phi} \setminus (x_0, P_{x_0})} P_x h_x \ell(\|x\|)}{P_{x_0} \ell(r_0)} \right) \right] \\ &= \exp \left( -\frac{\theta W}{P_{x_0} \ell(r_0)} \right) \prod_{(x, P_x) \in \tilde{\Phi} \setminus (x_0, P_{x_0})} \frac{1}{1 + \frac{\theta P_x \ell(\|x\|)}{P_{x_0} \ell(r_0)}} \\ &= \exp \left( -\frac{\theta W}{P_{x_0} \ell(r_0)} - \sum_{(x, P_x) \in \tilde{\Phi} \setminus (x_0, P_{x_0})} \ln \left( 1 + \frac{\theta P_x \ell(\|x\|)}{P_{x_0} \ell(r_0)} \right) \right) \quad (27) \\ &\stackrel{(a)}{\geq} \exp \left( -\frac{\theta W}{P_{x_0} \ell(r_0)} - \frac{\theta}{P_{x_0} \ell(r_0)} \sum_{(x, P_x) \in \tilde{\Phi} \setminus (x_0, P_{x_0})} P_x \ell(\|x\|) \right) \\ &\stackrel{(b)}{\geq} \exp \left( -\frac{\theta W}{P_{x_0} \ell(r_0)} - \frac{\theta(A_\ell - P_{x_0} \ell(r_0))}{P_{x_0} \ell(r_0)} \right) \\ &= \exp \left( -\frac{\theta(W + A_\ell)}{P_{x_0} \ell(r_0)} + \theta \right), \quad \mathbb{P}\text{-a.s.}, \end{aligned}$$

where (a) follows from the inequality  $\ln(1+x) < x$  for  $x > 0$ , and (b) follows from (13).  $\square$

The result established in the theorem highlights the impact of shot-noise regulation on link success probability in Rayleigh fading channels. The derived lower bound for the SINR demonstrates that effective ball regulation and interference management can significantly enhance network performance, even in the presence of fading.

### III. DETERMINISTIC PERFORMANCE GUARANTEES WITH HETEROGENEOUS TRAFFIC

In an irregularly deployed wireless network, nearby links may be in close proximity, leading to significant interference and degraded performance. To ensure quality of service for diverse users, we can maintain a minimum distance between nodes during deployment or implement medium access protocols such as CSMA to isolate links spatially. The key question is how to establish such isolation using the regulations proposed in the previous section to ensure the required performance.

In the following discussion, we consider mutual exclusion among transmitters and employ the MHCPP model (see Fig. 3). This model enforces mutually exclusive regulations for

transmitter deployment, ensuring that the distance between any two transmitters is at least the hardcore distance  $H$ .

We utilize a type II MHCPP, which is more practical for modeling CSMA protocols compared to type I. We will further explore the relationship between the mutually exclusive of the MHCPP and the regulations introduced in the previous section.

In our analysis, we examine all links within large-scale wireless networks characterized by heterogeneous traffic. The locations of transmitters serving users with varying requirements are modeled as independent MHCPPs, thinned from PPPs with different hardcore distances. We assume that the retained links in the network are always active, enabling us to derive worst-case bounds without considering the impact of queuing. Our primary interest is whether we can guarantee the requirements of different classes of links through the introduction of regulations.

Assume that there are  $M$  classes of links in a large wireless network, each with different target SINR thresholds  $\theta_1, \theta_2, \dots, \theta_M$ , where  $\theta_1 > \theta_2 > \dots > \theta_M > 0$ . We denote the type II MHCPP corresponding to the  $i$ -th link class by a stationary and ergodic point process  $\Phi_i$  on  $\mathbb{R}^2$ , with a hardcore distance of  $H_i$ . The superposition of the point processes for different link classes is defined as  $\Phi \triangleq \bigcup_{i=1}^M \Phi_i$ . It is important to note that the point processes  $\Phi_i$  are assumed to be independent of each other.

Let  $\Psi_i$  denote the point process corresponding to the receivers, which is jointly stationary and ergodic with  $\Phi_i$ . The link distance  $r_0$  between each receiver and its dedicated transmitter is fixed. For simplicity, we assume that the bandwidth is normalized to 1. The transmit power of all transmitters within the  $i$ -th link class is constant and denoted by  $P_i$ .

In this section, we hypothesize that the channels within the small-scale wireless network models are characterized by two cases: Rayleigh fading and the absence of fading. Using a bounded, non-increasing, continuous, and integrable function  $\ell(r)$  as the path loss function, we can express the SINR for the  $i$ -th link class as:

$$\text{SINR}_i = \frac{P_i h_{x_0} \ell(r_0)}{I + W}, \quad (28)$$

where  $I$  represents the interference power from other signals in the network, including contributions from transmitters in the  $i$ -th class as well as those in other classes.  $h_{x_0}$  denotes the small-scale fading coefficient from a transmitter located at position  $x_0$  to its corresponding receiver.

#### A. Performance Guarantee

Since the MHCPP is a stationary point process, we can place the user of the  $i$ -th class at the origin without loss of generality and denote its dedicated transmitter by  $x_0 \in \Phi_i$ . In a network with  $M$  classes of users, the total interference received by the user at the origin can be expressed as:

$$I_i = \sum_{j=1}^M \sum_{x \in \Phi_j} P_j h_x \ell(\|x\|) - P_{x_0} h_{x_0} \ell(r_0). \quad (29)$$

**Theorem 4.** *In a heterogeneous scenario modeled by  $M$  MHCPPs and in the absence of channel fading (i.e.,  $h_x \equiv 1$ ),*

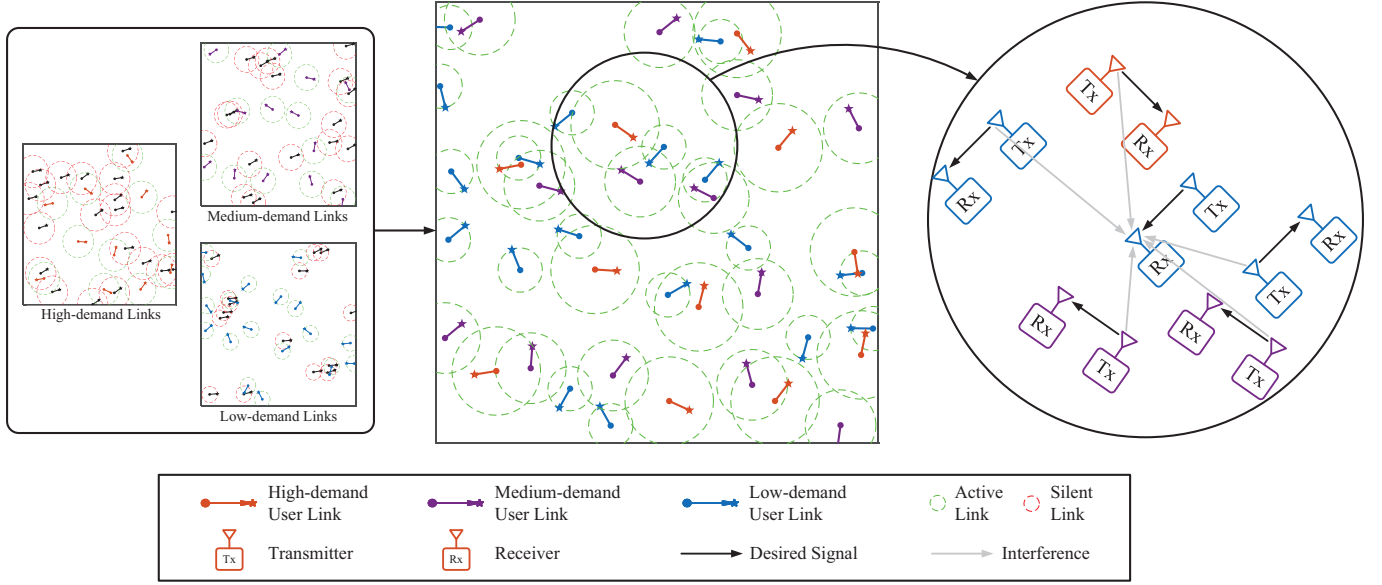


Fig. 3. Diagram of a bipolar network. Solid dots within dashed circles represent transmitters, distributed as a PPP with intensity  $\lambda = 0.3$ . Stars mark the uniformly distributed receiver locations. Transmitters and receivers are separated by a fixed distance  $r_0 = 0.5$  meters. The network employs an MHCPP of type II for the different demand links respectively, thinning the PPP where retained transmitters are shown in green dashed circles. Active links are color-coded to indicate user SINR thresholds: orange links represent high threshold users with hardcore distance  $H_1 = 1$  meter, purple links represent medium threshold users with  $H_2 = 0.8$  meters and blue for low threshold users with  $H_3 = 0.5$  meters.

the interference experienced by a user in the  $i$ -th class can be bounded as

$$I_i \leq \sum_{j=1}^M A_{\ell,j} - P_i \ell(r_0), \quad (30)$$

where the lower bound for the SINR experienced by a user in the  $i$ -th class is given by

$$\text{SINR}_i \geq \frac{P_i \ell(r_0)}{\sum_{j=1}^M A_{\ell,j} - P_i \ell(r_0)}, \quad (31)$$

and  $A_{\ell,j}$  represents the contribution from the  $j$ -th class to the overall interference, defined as

$$A_{\ell,j} \triangleq \sigma_j \ell(0) + \rho_j \int_0^\infty \ell(r) dr + 2\nu_j \int_0^\infty r \ell(r) dr, \quad (32)$$

where  $A_{\ell,j}$  provides the asymptotic upper bound on the total weighted sum of all points in  $\Phi_j$ , weighted by the function  $\ell$  and the transmit power  $P_j$ . Here,  $\sigma_j = P_j$ ,  $\rho_j = \frac{2\pi P_j}{\sqrt{12}H_j}$ , and  $\nu_j = \frac{\pi P_j}{\sqrt{12}H_j^2}$ .

*Proof.* Since the transmitters of the  $j$ -th class of links form a type II MHCPP with a hardcore distance  $H_j$  and constant transmit power  $P_j$ , applying Lemma 2 shows that the marked point process  $\tilde{\Phi}_j \triangleq \{(x, P_x) : x \in \Phi_j, P_x = P_j\}$  is strongly  $\left(P_j, \frac{2\pi P_j}{\sqrt{12}H_j}, \frac{\pi P_j}{\sqrt{12}H_j^2}\right)$ -ball regulated. Due to the equivalence between strong ball regulation and strong shot-noise regulation established in Theorem 1, we conclude that the marked point process  $\tilde{\Phi}_j$  is also strongly  $\left(P_j, \frac{2\pi P_j}{\sqrt{12}H_j}, \frac{\pi P_j}{\sqrt{12}H_j^2}\right)$ -shot-noise regulated.

In a scenario without channel fading (i.e.,  $h_x \equiv 1$ ), the interference experienced by a user in the  $i$ -th class can be

bounded using (13) as (30). Given this upper bound on interference, we can derive further lower bounds for link SINR in (31).  $\square$

The theorem emphasizes the critical relationship between interference and SINR in heterogeneous wireless networks modeled by multiple MHCPPs. In particular, the proof can also be approached from a different perspective.

Consider that the transmitters associated with the  $i$ -th link class are distributed as a type II MHCPP  $\Phi_i$  on  $\mathbb{R}^2$  with a minimum separation distance (hardcore distance)  $H_i$ . Since we have established that each marked MHCPP is  $\left(P_j, \frac{2\pi P_j}{\sqrt{12}H_j}, \frac{\pi P_j}{\sqrt{12}H_j^2}\right)$ -ball regulated in Lemma 2, we can invoke Lemma 3 to demonstrate that the superposition of the  $M$  marked MHCPPs, defined as  $\tilde{\Phi} = \bigcup_{i=1}^M \tilde{\Phi}_i$ , is also a ball regulated point process.

**Lemma 3.** *The superposition point process  $\tilde{\Phi}$  of  $M$  marked MHCPPs is strongly  $(\sigma, \rho, \nu)$ -ball regulated, where  $\sigma = \sum_{i=1}^M P_i$ ,  $\rho = \sum_{i=1}^M \frac{2\pi P_i}{\sqrt{12}H_i}$ , and  $\nu = \sum_{i=1}^M \frac{\pi P_i}{\sqrt{12}H_i^2}$ .*

*Proof.* From Lemma 2, we know that the marked point process with all points construing a type II MHCPP  $\Phi_i$  with hardcore distance  $H_i$  and with transmit power mark  $P_i$  is strongly  $\left(P_i, \frac{2\pi P_i}{\sqrt{12}H_i}, \frac{\pi P_i}{\sqrt{12}H_i^2}\right)$ -ball regulated.

By applying Lemma 1, we conclude that the superposition marked point process  $\tilde{\Phi}$  is strongly  $(\sigma, \rho, \nu)$ -ball regulated.  $\square$

Thus, utilizing Theorem 3, this alternative approach also confirms the results presented in Theorem 4.

From Lemma 3, we derive that the total power allocated to all transmitters within  $B(o, r)$  can be expressed as

$$P_{\text{total}}(o, r) \leq \sum_{i=1}^M P_i + \sum_{i=1}^M \frac{2\pi}{\sqrt{12}} \left( \frac{P_i}{H_i} \right) r + \sum_{i=1}^M \frac{\pi}{\sqrt{12}} \left( \frac{P_i}{H_i^2} \right) r^2. \quad (33)$$

This inequality provides an upper bound on the total transmission power of the network within  $B(o, r)$ .

**Theorem 5.** *In a heterogeneous scenario modeled by  $M$  MHCPPs and considering Rayleigh fading, the link success probability  $P_s(\theta_i | \tilde{\Phi})$  for the  $i$ -th class satisfies*

$$P_s(\theta_i | \tilde{\Phi}) \geq \exp \left( -\frac{\theta_i W}{P_i \ell(r_0)} - \sum_{j=1}^M A_{\tilde{\ell}_{ij}} \right), \quad \mathbb{P}\text{-a.s.}, \quad (34)$$

where  $A_{\tilde{\ell}_{ij}}$  is defined as

$$A_{\tilde{\ell}_{ij}} \triangleq \sigma_j \tilde{\ell}_{ij}(0) + \rho_j \int_0^\infty \tilde{\ell}_{ij}(r) dr + 2\nu_j \int_0^\infty r \tilde{\ell}_{ij}(r) dr, \quad (35)$$

and  $\tilde{\ell}_{ij}(r)$  is given by

$$\tilde{\ell}_{ij}(r) \triangleq \ln \left( 1 + \frac{\theta_i P_j \ell(r)}{P_i \ell(r_0)} \right). \quad (36)$$

*Proof.* Considering the case with Rayleigh fading channels and different target SINR thresholds  $\theta_i > 0$  for each class of links, the link success probability for the  $i$ -th class can be expressed as

$$\begin{aligned} P_s(\theta_i | \tilde{\Phi}) &\triangleq \mathbb{P}(\text{SINR}_i > \theta_i | \tilde{\Phi}) \\ &= \mathbb{P} \left[ \frac{P_i h_{x_0} \ell(r_0)}{I + W} > \theta_i \middle| \tilde{\Phi} \right], \end{aligned} \quad (37)$$

where  $\tilde{\Phi} = \bigcup_{i=1}^M \tilde{\Phi}_i$  represents the superposition of marked point processes for all  $M$  classes of links.

The link success probability for the  $i$ -th class user in a large-scale wireless network can be calculated as follows.

$$\begin{aligned} P_s(\theta_i | \tilde{\Phi}) &= \exp \left( -\frac{\theta_i W}{P_i \ell(r_0)} \right) \\ &\times \mathbb{E} \left[ \exp \left( -\frac{\theta_i \sum_{j=1}^M \sum_{x \in \tilde{\Phi}_j \setminus \{x_0\}} P_j h_x \ell(\|x\|)}{P_i \ell(r_0)} \right) \middle| \tilde{\Phi} \right]. \end{aligned} \quad (38)$$

This can be further simplified to

$$\begin{aligned} P_s(\theta_i | \tilde{\Phi}) &= \exp \left( -\frac{\theta_i W}{P_i \ell(r_0)} \right) \\ &\times \prod_{j=1}^M \prod_{(x, P_x) \in \tilde{\Phi}_j \setminus (x_0, P_{x_0})} \frac{1}{1 + \frac{\theta_i P_j \ell(\|x\|)}{P_i \ell(r_0)}} \\ &= \exp \left( -\frac{\theta_i W}{P_i \ell(r_0)} - \sum_{j=1}^M \sum_{(x, P_x) \in \tilde{\Phi}_j \setminus (x_0, P_{x_0})} \ln \left( 1 + \frac{\theta_i P_j \ell(\|x\|)}{P_i \ell(r_0)} \right) \right) \\ &= \exp \left( -\frac{\theta_i W}{P_i \ell(r_0)} - \sum_{j=1}^M \sum_{(x, P_x) \in \tilde{\Phi}_j \setminus (x_0, P_{x_0})} \tilde{\ell}_{ij}(r) \right), \end{aligned} \quad (39)$$

where  $\tilde{\ell}_{ij}(r)$  is defined in (36), which is non-increasing, monotonic, and bounded.

Since  $\tilde{\Phi}_j$  is  $(\sigma_j, \rho_j, \nu_j)$ -ball regulated with  $\sigma_j = P_j$ ,  $\rho_j = \frac{2\pi P_j}{\sqrt{12} H_j}$ , and  $\nu_j = \frac{\pi P_j}{\sqrt{12} H_j^2}$ , by the equivalence established in Theorem 1,  $\tilde{\Phi}_j$  is also  $(\sigma_j, \rho_j, \nu_j)$ -shot-noise regulated.

Therefore, combining this with (13) and (14), we obtain the following bound:

$$\sum_{(x, P_x) \in \tilde{\Phi}_j \setminus (x_0, P_{x_0})} \tilde{\ell}_{ij}(r) \leq A_{\tilde{\ell}_{ij}}, \quad (40)$$

where  $A_{\tilde{\ell}_{ij}}$  is defined in (35).

Substituting (40) into (39), we derive the lower bound given in (34). This derivation demonstrates that the SINR exceeds the threshold  $\theta_i$  with a probability constrained by noise and interference, thereby providing a lower bound on the link success probability for  $i$ -th class users by considering the combined effects of power control and shot-noise regulation.  $\square$

Theorem 5 provides lower bounds on the link success probability for each of the  $M$  classes of links in the network. To derive an overall lower bound on the link success probability across all links, we define the minimum link success probability, denoted as  $P_{s, \min}$ , as:

$$P_{s, \min} \triangleq \min_{i \in [1, M]} P_s(\theta_i | \tilde{\Phi}). \quad (41)$$

Using this definition, we present the following corollary, which establishes a lower bound on the link success probability across all links in the network.

**Corollary 2.** *In a heterogeneous network scenario modeled by  $M$  MHCPPs, under Rayleigh fading conditions, the overall link success probability across all links satisfies the following inequality:*

$$P_{s, \min} \geq \min_{i \in [1, M]} \exp \left( -\frac{\theta_i W}{P_i \ell(r_0)} - \sum_{j=1}^M A_{\tilde{\ell}_{ij}} \right), \quad \mathbb{P}\text{-a.s.}, \quad (42)$$

where  $A_{\tilde{\ell}_{ij}}$  is defined in (35).

*Proof.* The result is directly derived from Theorem 5. By applying the minimization operation to both sides of inequality (34) over all  $i \in [1, M]$ , we obtain the desired bound.  $\square$

**Example 1.** *Theorem 5 is applicable to a general path loss function  $\ell(\cdot)$ . As a specific example, when the path loss function is given by  $\ell(r) = \min\{1, r^{-\alpha}\}$ , we can explicitly calculate  $A_{\tilde{\ell}_{ij}}$  as*

$$\begin{aligned} A_{\tilde{\ell}_{ij}} &= \sigma_j \ln \left( 1 + \frac{P_j \theta_i}{P_i \ell(r_0)} \right) \\ &+ \rho_j \frac{\alpha P_j \theta_i}{(\alpha - 1) P_i \ell(r_0)} {}_2F_1 \left( 1 - \frac{1}{\alpha}, 1; 2 - \frac{1}{\alpha}; -\frac{P_j \theta_i}{P_i \ell(r_0)} \right) \\ &+ \nu_j \frac{\alpha P_j \theta_i}{(\alpha - 2) P_i \ell(r_0)} {}_2F_1 \left( 1 - \frac{2}{\alpha}, 1; 2 - \frac{2}{\alpha}; -\frac{P_j \theta_i}{P_i \ell(r_0)} \right), \end{aligned} \quad (43)$$

where  ${}_2F_1(\cdot)$  denotes the Gauss hypergeometric function.

To arrive at this result, we substitute  $\ell(r) = \min\{1, r^{-\alpha}\}$  into the general expression of  $A_{\tilde{\ell}_{ij}}$  in (35), which yields:

$$\begin{aligned} A_{\tilde{\ell}_{ij}} &= \sigma_j \ln \left( 1 + \frac{P_j \theta_i}{P_i \ell(r_0)} \right) + \rho_j \ln \left( 1 + \frac{P_j \theta_i}{P_i \ell(r_0)} \right) \\ &+ \rho_j \int_1^\infty \ln \left( 1 + \frac{P_j \theta_i r^{-\alpha}}{P_i \ell(r_0)} \right) dr \\ &+ \nu_j \ln \left( 1 + \frac{P_j \theta_i}{P_i \ell(r_0)} \right) + 2\nu_j \int_1^\infty r \ln \left( 1 + \frac{P_j \theta_i r^{-\alpha}}{P_i \ell(r_0)} \right) dr. \end{aligned} \quad (44)$$

The first integral term can be evaluated as

$$\begin{aligned} \int_1^\infty \ln \left( 1 + \frac{P_j \theta_i r^{-\alpha}}{P_i \ell(r_0)} \right) dr &= -\ln \left( 1 + \frac{P_j \theta_i}{P_i \ell(r_0)} \right) \\ &+ \frac{\alpha P_j \theta_i}{(\alpha - 1) P_i \ell(r_0)} {}_2F_1 \left( 1 - \frac{1}{\alpha}, 1; 2 - \frac{1}{\alpha}; -\frac{P_j \theta_i}{P_i \ell(r_0)} \right). \end{aligned} \quad (45)$$

Similarly, the second integral term evaluates to

$$\begin{aligned} \int_1^\infty r \ln \left( 1 + \frac{P_j \theta_i r^{-\alpha}}{P_i \ell(r_0)} \right) dr &= -\frac{1}{2} \ln \left( 1 + \frac{P_j \theta_i}{P_i \ell(r_0)} \right) \\ &+ \frac{\alpha P_j \theta_i}{2(\alpha - 2) P_i \ell(r_0)} {}_2F_1 \left( 1 - \frac{2}{\alpha}, 1; 2 - \frac{2}{\alpha}; -\frac{P_j \theta_i}{P_i \ell(r_0)} \right). \end{aligned} \quad (46)$$

Substituting these results back into the expression for  $A_{\tilde{\ell}_{ij}}$  completes the derivation of (43).

Theorem 5 provides a deterministic lower bound for the link success probability in a large wireless network modeled by  $M$  MHCPPs, ensuring a minimum success probability for all links.

However, when the SINR threshold for different tiers are the same, i.e.  $\theta_i = \theta$  for all  $i$ , a simpler and looser lower bound can be derived with fewer steps, as shown in the following theorem.

**Corollary 3.** *In a heterogeneous network scenario with  $M$  MHCPPs and Rayleigh fading, a simplified lower bound for the link success probability  $P_s(\theta_i | \tilde{\Phi})$  of the  $i$ -th class is:*

$$P_s(\theta_i | \tilde{\Phi}) \geq \exp \left( -\frac{\theta_i(W + A_\ell)}{P_{x_0} \ell(r_0)} + \theta_i \right), \quad \mathbb{P}\text{-a.s.} \quad (47)$$

where  $A_\ell$  is defined in equation (14), with  $\sigma = \sum_{i=1}^M P_i$ ,  $\rho = \sum_{i=1}^M \frac{2\pi P_i}{\sqrt{12}H_i}$ , and  $\nu = \sum_{i=1}^M \frac{\pi P_i}{\sqrt{12}H_i^2}$ .

*Proof.* Since  $\tilde{\Phi}$  is the superposition of  $M$  MHCPPs with transmit power marks, where each individual marked point process  $\tilde{\Phi}_i$  is  $\left( P_i, \frac{2\pi P_i}{\sqrt{12}H_i}, \frac{\pi P_i}{\sqrt{12}H_i^2} \right)$ -ball regulated, we apply Lemma 3 to conclude that the superposition marked point process  $\tilde{\Phi}$  is strongly  $(\sigma, \rho, \nu)$ -ball regulated, where

$$\sigma = \sum_{i=1}^M P_i, \quad \rho = \sum_{i=1}^M \frac{2\pi P_i}{\sqrt{12}H_i}, \quad \text{and} \quad \nu = \sum_{i=1}^M \frac{\pi P_i}{\sqrt{12}H_i^2}. \quad (48)$$

Using Theorem 1, we then conclude that the superposition marked point process  $\tilde{\Phi}$  is strongly  $(\tilde{\sigma}, \tilde{\rho}, \tilde{\nu})$ -shot-noise regulated.

Finally, applying Theorem 3 yields the simplified lower bound for the link success probability as stated.  $\square$

## B. Requirement-based Power Control

To ensure that the requirements of different link classes are met, we consider a power control scheme that allocates distinct transmit powers  $P_i$  to the transmitters of the  $i$ -th link class based on their respective SINR requirements  $\theta_i$ .

This power control strategy is designed to meet the quality of service requirements of each user class by distributing power uniformly within the same class, while varying it across classes according to their SINR thresholds. Classes with higher SINR requirements are allocated more power to meet their stringent quality of service needs. This approach defines our requirement-based power control scheme.

**Definition 5.** ( $\beta$ -Power Control). *For a given constant  $\beta > 0$ , the power  $P$  allocated to a link with a target SINR threshold  $\theta$  is defined by:*

$$P = \ln(1 + \beta\theta). \quad (49)$$

This allocation formula applies to all transmitters for any given SINR threshold  $\theta$ .

According to Definition 5, the power allocated to the  $i$ -th class is determined by its designated SINR threshold  $\theta_i$ . Specifically, the allocated power is given by:

$$P_i = \ln(1 + \beta\theta_i), \quad (50)$$

where  $\theta_i$  represents the SINR requirement necessary for users in the  $i$ -th class to achieve satisfactory service quality. This power control scheme is motivated by Shannon's theorem, which indicates that an increase in the SINR threshold corresponds to a logarithmic increase in the achievable data rate.

Therefore, the transmit power for each transmitter is calculated according to the SINR thresholds assigned to different user classes. Users with higher SINR requirements are allocated more power, while those with lower requirements receive less. The primary challenge lies in determining whether this power control scheme can improve performance lower bounds or guarantee enhanced performance for all links in the wireless network.

In the following discussion, we explore the impact of the  $\beta$ -power control strategy on network performance. We will examine how this strategy influences the distribution and utilization of power across different classes of users within the network. Additionally, we aim to derive a lower bound on the link success probability for networks with multi-requirement users, demonstrating how strategic power control can enhance overall network success probability.

The total power consumption for all transmitters within the network is given by

$$P_{\text{total}}(o, r) \leq \sum_{i=1}^M \left( 1 + \frac{2\pi r}{\sqrt{12}H_i} + \frac{\pi r^2}{\sqrt{12}H_i^2} \right) \ln(1 + \beta\theta_i). \quad (51)$$

By substituting the transmit power (50) into Theorem 5, we derive the following corollary, which provides the lower bound for the link success probability under the  $\beta$ -power control strategy.

**Corollary 4.** *In a heterogeneous network scenario modeled by  $M$  MHCPPs and considering Rayleigh fading, the link success*

probability  $P_s(\theta_i | \tilde{\Phi})$  for the  $i$ -th class with the  $\beta$ -power control strategy is given by

$$P_s(\theta_i | \tilde{\Phi}) \geq \exp\left(-\frac{\theta_i W}{\ln(1 + \beta\theta_i)\ell(r_0)} - \sum_{j=1}^M A_{\tilde{\ell}_{ij}}\right), \mathbb{P}\text{-a.s.}, \quad (52)$$

where  $A_{\tilde{\ell}_{ij}}$  is defined in (35), and  $\tilde{\ell}_{ij}(r)$  is given by

$$\tilde{\ell}_{ij}(r) \triangleq \ln\left(1 + \frac{\theta_i \ln(1 + \beta\theta_j)\ell(r)}{\ln(1 + \beta\theta_i)\ell(r_0)}\right). \quad (53)$$

#### IV. NUMERICAL RESULTS

In this section, we delve into the performance evaluation of a wireless network serving two distinct classes of users, categorized based on their SINR thresholds: high-requirement and low-requirement. We conduct simulations to assess the practical effectiveness of our theoretical models and to compare the simulated outcomes with the theoretically derived lower bounds of link success probability. The simulation environment is configured with transmitters arranged in a triangular lattice within a circular region of radius  $r = 100$  meters, adhering to hardcore distances  $H_1 = 1$  meter for high-requirement users and  $H_2 = 1$  meter for low-requirement users. This configuration ensures that the distribution of transmitters corresponding to users of different requirements is mutually independent and unaffected by users of other requirements. However, the  $i$ -th class of links are still subject to interference from the transmitters corresponding to users of other classes. The marked point process governing the locations of the transmitters  $\Phi_i$  is strongly regulated by a  $(1, 2\pi/(\sqrt{12}H_i), \pi/(\sqrt{12}H_i^2))$ -ball regulation model, which provides a basis for calculating theoretical lower bounds and conducting rigorous simulations. The simulation parameters include SINR thresholds  $\theta_1$  and  $\theta_2$  for high-requirement and low-requirement users, respectively, assuming  $\theta_1 > \theta_2 > 0$ . Additional parameters are set as follows: power factor  $\beta = 1$ , noise power  $W = 0$  and a distance  $r_0 = 1$  meter between users and their dedicated transmitters. The path loss function is defined as  $\ell(r) = \min\{1, r^{-\alpha}\}$ . In subsequent analyses, we set the path loss exponent, denoted as  $\alpha$ , to 4. We define the reference threshold as  $\theta$ , setting  $\theta_1$  equal to  $\theta$  and  $\theta_2$  to  $\theta - 3$  dB.

Fig. 4 illustrates the variation in the lower bounds of link success probability for two classes of users as their SINR thresholds ( $\theta_1$  and  $\theta_2$ ) change. This figure includes both simulation results and theoretical calculations for high-requirement users and low-requirement users, respectively. For users with the same requirement, the vertical gap represents the differences in the link success probability lower bound between simulation results and theoretical calculations. This discrepancy was mainly influenced by the point process modeling the locations of transmitters and the path loss function. The horizontal gap indicates the difference in SINR threshold required to achieve the desired link success probability. In particular, when the link success probability exceeds 0.8, the horizontal deviations between the simulation results and the theoretical lower bounds are less than 3 dB for high-requirement users and 2 dB for low-requirement users. As the

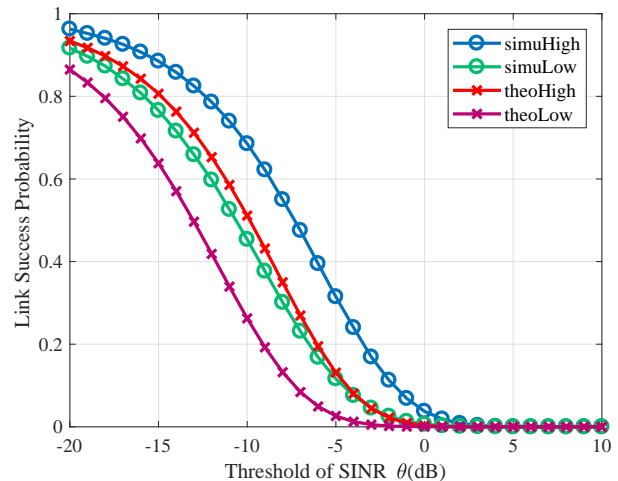


Fig. 4. Link success probability vs. the changes of the users' thresholds.

SINR threshold increases, the lower bound of link success probability decreases. This indicates that higher user demands make it increasingly difficult to meet all user requirements. Low-requirement users suffer from lower link success probability than high-requirement users because their dedicated transmitters are allocated less power, leading to a lower SINR, thus necessitating a lower threshold to satisfy their requirements.

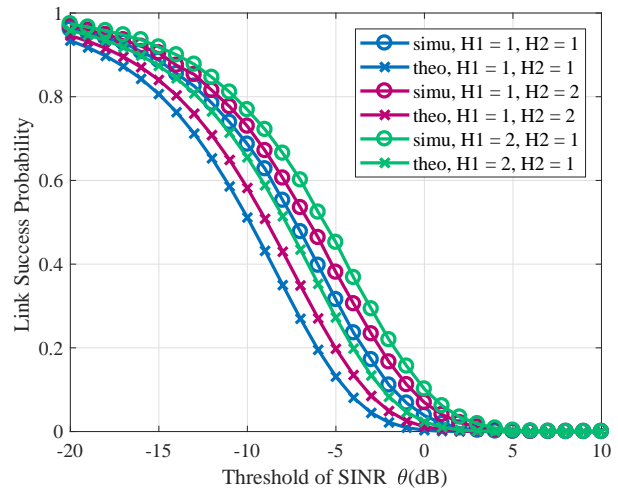


Fig. 5. Link success probability with different hardcore distances

Fig. 5 shows the impact of different hardcore distances on the link success probability lower bound for high-requirement users. This analysis considers scenarios where transmitters for high-requirement and low-requirement users are positioned at distinct hardcore distances. Specifically, when the hardcore distances  $H_1$  and  $H_2$  are set to 1 meter, the link success probability lower bound reaches its minimum. This decrease is attributed to the increase density of transmitters, which intensifies the interference within the wireless network. Furthermore, when the hardcore distances are set as  $H_1 = 2$  meters and  $H_2 = 1$  meter, a higher link success probability lower bound

is observed. This improvement can be attributed not only to the reduced density of transmitters regulated by the hardcore distance, but also to the power control strategy, which allocates less power to low-requirement transmitters, thereby reducing the overall level of interference within the wireless network.

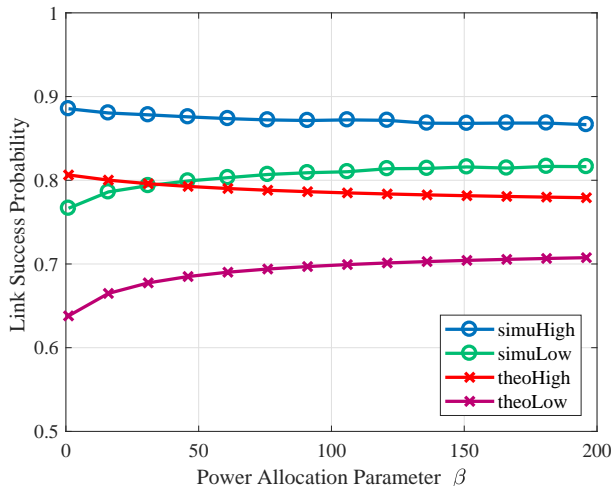


Fig. 6. Link success probability vs. the changes of  $\beta$

In Fig. 6, the impact of the parameter  $\beta$  within the  $\beta$ -power control strategy on link success probability lower bound, with  $\beta$  varying from 1 to 200 and  $\theta$  set at  $-15$  dB, is illustrated. It shows a clear increase in the link success probability lower bound for low-requirement users as  $\beta$  increases, which coincides with a decrease in link success probability lower bound for high-requirement users. Furthermore, there is no optimal  $\beta$  value that achieves higher link success probability lower bound for both high-requirement and low-requirement users simultaneously.

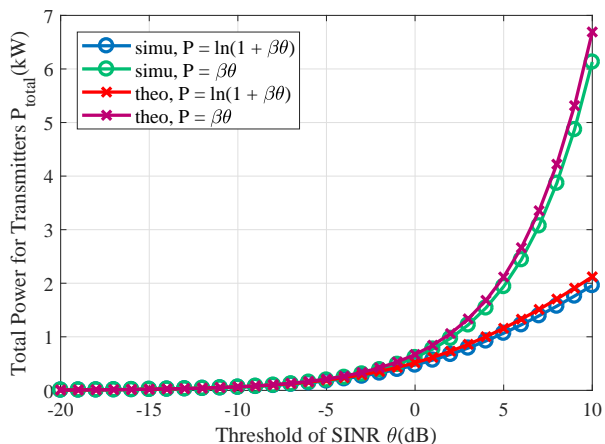


Fig. 7. Total Power for Transmitters vs. the Changes of  $\theta$

Fig. 7 examines the variations in total power consumption of the transmitters with changes in the SINR threshold  $\theta$ , comparing two power control strategies:  $P = \ln(1 + \beta\theta)$  as mentioned in Def. 5 and  $P = \beta\theta$ . The theoretical results provide the upper bound on  $P_{\text{total}}(o, r)$ , as derived from (33). The

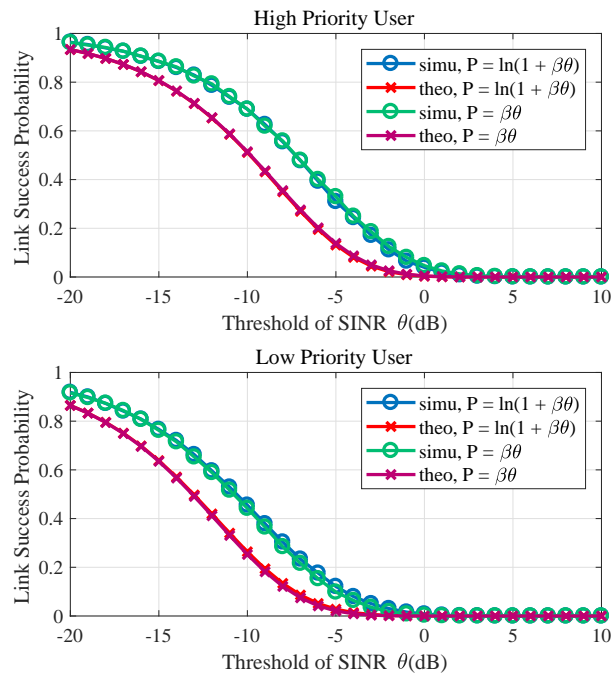


Fig. 8. Link success probability lower bound vs. the changes of  $\theta$

proposed power control strategy consumes less total power under all SINR thresholds, and the power difference continues to increase as the SINR threshold increases. This implies that utilizing the  $\beta$ -power control strategy is more effective to reduce power consumption. Fig. 8 presents a comparison of the link success probability lower bounds for high-requirement and low-requirement users under two different power control strategies, given equal total power for transmitters. The figures indicate that using the allocation strategy  $P = \ln(1 + \beta\theta)$  slightly enhances the link success probability lower bound for low-requirement users, with no marked impact on high-requirement users.

## V. CONCLUSION

This work introduces a novel regulatory framework to constrain the total transmit power and the aggregated interference in large-scale wireless networks. As an example, we utilize the Matérn II method to demonstrate how these regulations can be algorithmically implemented. Our work provides computable bounds on link performance suitable for various user requirements, establishing a robust analytical framework for evaluating network efficiency. Monte Carlo simulations validated our approach across different user classes, underscoring the practical relevance and efficacy of our regulatory strategies in real-world settings.

Looking ahead, our research will explore the integration of queuing theory in the time domain with spatial-temporal network calculus to enhance service quality across different requirement levels. We also plan to assess the impacts of environmental factors such as shadowing, exposure to radio frequency electromagnetic fields, and strategies such as dynamic power control and load balancing on network

performance, aiming to refine and extend the performance guarantees essential for future wireless network deployments.

## REFERENCES

- [1] X. Zhou, Y. Zhong, and K. Feng, "Service Guarantee in Multi-Priority Traffic: A Spatial Network Calculus Perspective," *International Symposium on Modeling and Optimization in Mobile, Ad Hoc, and Wireless Networks (WiOpt)*, 2024.
- [2] A. Nasrallah, A. S. Thyagaturu, Z. Alharbi, C. Wang, X. Shao, M. Reisslein, and H. ElBakoury, "Ultra-Low Latency (ULL) Networks: The IEEE TSN and IETF DetNet Standards and Related 5G ULL Research," *IEEE Communications Surveys and Tutorials*, vol. 21, no. 1, pp. 88–145, 2019.
- [3] F. Song, L. Li, I. You, and H. Zhang, "Enabling Heterogeneous Deterministic Networks with Smart Collaborative Theory," *IEEE Network*, vol. 35, no. 3, pp. 64–71, 2021.
- [4] R. L. Cruz, "A calculus for network delay. I. Network elements in isolation," *IEEE Trans. Inf. Theory*, vol. 37, no. 1, pp. 114–131, 1991.
- [5] —, "A calculus for network delay. II. Network analysis," *IEEE Trans. Inf. Theory*, vol. 37, no. 1, pp. 132–141, 1991.
- [6] K. Feng and F. Baccelli, "Spatial Network Calculus and Performance Guarantees in Wireless Networks," *IEEE Trans. Wirel. Commun.*, vol. 23, no. 5, pp. 5033–5047, 2024.
- [7] M. Haenggi, *Stochastic geometry for wireless networks*. Cambridge University Press, 2012.
- [8] J. G. Andrews, F. Baccelli, and R. K. Ganti, "A Tractable Approach to Coverage and Rate in Cellular Networks," *IEEE Trans. on Commun.*, vol. 59, no. 11, pp. 3122–3134, 2011.
- [9] B. Błaszczyszyn and C. Hirsch, "Optimal stationary markings," *Stochastic Processes and their Applications*, vol. 138, pp. 153–185, 2021. [Online]. Available: <https://www.sciencedirect.com/science/article/pii/S0304414921000508>
- [10] Y. Zhong, Z. Chen, T. Han, and X. Ge, "Spatio-Temporal Interference Correlation: Influence of Deployment Patterns and Traffic Dynamics," *IEEE Transactions on Communications*, 2024, in press.
- [11] Y. Hwang and S. Oh, "A study on ultra-reliable and low-latency communication technologies for 5G & 6G services," in *13th International Conference on Information and Communication Technology Convergence (ICTC)*. IEEE, 2022, pp. 1207–1209.
- [12] Y. Zhong and X. Ge, "Toward 6G Carbon-Neutral Cellular Networks," *IEEE Network*, vol. 38, no. 5, pp. 174–181, 2024.
- [13] Y. Zhong, G. Mao, X. Ge, and F.-C. Zheng, "Spatio-temporal modeling for massive and sporadic access," *IEEE Journal on Selected Areas in Communications*, vol. 39, no. 3, pp. 638–651, 2020.
- [14] H. Q. Nguyen, F. Baccelli, and D. Kofman, "A stochastic geometry analysis of dense IEEE 802.11 networks," in *26th IEEE International Conference on Computer Communications (IEEE INFOCOM)*, 2007, pp. 1199–1207.
- [15] M. Haenggi, "Mean Interference in Hard-Core Wireless Networks," *IEEE Commun. Lett.*, vol. 15, no. 8, pp. 792–794, Aug. 2011.
- [16] T. V. Nguyen, F. Baccelli, K. Zhu, S. Subramanian, and X. Wu, "A performance analysis of CSMA based broadcast protocol in VANETs," in *Proceedings of IEEE INFOCOM*, 2013, pp. 2805–2813.
- [17] K. V. Mishra, B. S. MR, and B. Ottersten, "Stochastic-geometry-Based interference modeling in automotive radars using matern hard-core process," in *IEEE Radar Conference (RadarConf)*, 2020, pp. 1–5.
- [18] M. Di Renzo, A. Zappone, T. T. Lam, and M. Debbah, "System-level modeling and optimization of the energy efficiency in cellular networks-A stochastic geometry framework," *IEEE Trans. Wirel. Commun.*, vol. 17, no. 4, pp. 2539–2556, 2018.
- [19] Z. Chen and Y. Zhong, "Characterizing Stability Regions in Wireless Networks With Hard-Core Spatial Constraints," *IEEE Wireless Comm. Lett.*, vol. 13, no. 8, pp. 2180–2184, 2024.
- [20] J. Miao, Z. Hu, K. Yang, and et al., "Joint power and bandwidth allocation algorithm with QoS support in heterogeneous wireless networks," *IEEE Commun. Lett.*, vol. 16, no. 4, pp. 479–481, 2012.
- [21] C. Liu, S. Zhang, X. Qin, and et al., "Utility-based resource allocation in OFDMA relay networks with service differentiation," in *IEEE Wireless Communications and Networking Conference (WCNC)*, 2011, pp. 72–77.
- [22] C.-S. Choi, "Modeling and Analysis of Priority-Based Distributed Access Control in Vehicular Networks," *IEEE Trans. Veh. Technol.*, vol. 71, no. 6, pp. 6848–6852, 2022.
- [23] N. Kumar, A. Ahmad, and D. K. Singh, "Priority Based Power Allocation in a Mobile Communication Network," in *IEEE International Conference on Power Energy, Environment and Intelligent Control (PEEIC)*, 2018, pp. 713–716.
- [24] A. Abdel-Hadi and C. Clancy, "A utility proportional fairness approach for resource allocation in 4G-LTE," in *International Conference on Computing, Networking and Communications (ICNC)*. IEEE, 2014, pp. 1034–1040.
- [25] J.-W. Lee, R. R. Mazumdar, and N. B. Shroff, "Opportunistic power scheduling for multi-server wireless systems with minimum performance constraints," in *IEEE INFOCOM*, vol. 2, 2004, pp. 1067–1077.
- [26] C.-S. Chang, "Performance guarantees in communication networks," *Eur. Trans. Telecommun.*, vol. 12, no. 4, pp. 357–358, 2001.
- [27] J.-Y. Le Boudec and P. Thiran, *Network calculus: a theory of deterministic queuing systems for the internet*. Springer, 2001.
- [28] M. Fidler and A. Rizk, "A Guide to the Stochastic Network Calculus," *IEEE Communications Surveys & Tutorials*, vol. 17, no. 1, pp. 92–105, 2015.
- [29] Y. Jiang, Y. Liu et al., *Stochastic network calculus*. Springer, 2008, vol. 1.
- [30] C.-S. Chang, *Performance guarantees in communication networks*. Springer Science and Business Media, 2012.
- [31] D.-K. Dang and A. Mifdaoui, "Timing Analysis of TDMA-Based Networks Using Network Calculus and Integer Linear Programming," in *IEEE 22nd International Symposium on Modelling, Analysis & Simulation of Computer and Telecommunication Systems*, 2014, pp. 21–30.
- [32] Y. Chen, H. Lu, L. Qin, C. Zhang, and C. W. Chen, "Statistical QoS Provisioning Analysis and Performance Optimization in xURLLC-Enabled Massive MU-MIMO Networks: A Stochastic Network Calculus Perspective," *IEEE Trans. on Wireless Commun.*, vol. 23, no. 7, pp. 8044–8058, 2024.
- [33] P. Cui, S. Han, X. Xu, J. Zhang, P. Zhang, and S. Ren, "End-to-End Delay Performance Analysis of Industrial Internet of Things: A Stochastic Network Calculus Perspective," *IEEE Internet of Things Journal*, vol. 11, no. 3, pp. 5374–5387, 2024.
- [34] M. Mei, M. Yao, Q. Yang, J. Wang, and R. R. Rao, "Stochastic Network Calculus Analysis of Spatial-Temporal Integrated Sensing and Communication Networks," *IEEE Trans. on Vehic. Tech.*, vol. 73, no. 6, pp. 9120–9124, 2024.
- [35] A. Bouillard, "Admission Shaping With Network Calculus," *IEEE Networking Lett.*, vol. 6, no. 2, pp. 115–118, 2024.
- [36] F. Baccelli, B. Błaszczyszyn et al., "Stochastic geometry and wireless networks: Volume II applications," *Foundations and trends® in networking*, vol. 4, no. 1–2, pp. 1–312, 2010.
- [37] M. Haenggi, R. K. Ganti et al., "Interference in large wireless networks," *Foundations and Trends® in Networking*, vol. 3, no. 2, pp. 127–248, 2009.
- [38] M. Haenggi, "The meta distribution of the SIR in Poisson bipolar and cellular networks," *IEEE Trans. Wirel. Commun.*, vol. 15, no. 4, pp. 2577–2589, 2015.
- [39] K. Feng and M. Haenggi, "Separability, asymptotics, and applications of the SIR meta distribution in cellular networks," *IEEE Trans. Wirel. Commun.*, vol. 19, no. 7, pp. 4806–4816, 2020.